Proceedings of ICONE12
12th International Conference on Nuclear Engineering
April 25-29, 2004, Arlington, Virginia USA

ICONE12-49293

EXPERIMENTAL STUDY ON POST-DRYOUT HEAT TRANSFER OF DISPERSED FLOW IN VERTICAL NARROW ANNULI

Aye Myint
State key Laboratory Of Multiphase Flow in power engineering, 710049, Xi'an, P. R. China,
uayemyint@yahoo.com

Wenxi Tian
State key Laboratory Of Multiphase Flow in power engineering, 710049, Xi'an, P. R. China,
wxtian_xjtu@163.com

Zhihui Li
Department of Nuclear & Thermal Power Engineering, Xi'an Jiaotong University, 710049, Xi'an, China

Suizheng Qiu
Department of Nuclear & Thermal Power Engineering, Xi'an Jiaotong University, 710049, Xi'an, China

Dounan Jia
Department of Nuclear & Thermal Power Engineering, Xi'an Jiaotong University, 710049, Xi'an,. China

Guanghui Su
Department of Nuclear & Thermal Power Engineering, Xi'an Jiaotong University, 710049, Xi'an, China

ABSTRACT: Forced convective post dryout heat transfer in narrow channel with 1.2 mm gap has been experimentally investigated with deionized water. The experiment was carried out with pressure ranging from 1.38 to 5.9 MPa and low mass velocity from 52.9 to 84.2 kg/m^2 s . The experimental data were compared with well known empirical correlations such as Groeneveld, Polimik, Miropolskiy and Slaughterbeck and it was found that these correlations could not predict very well in narrow annular gap at low mass velocity. Based on the experimental data, the heat transfer coefficient increases with increasing heat flux, mass flux and pressure. A new empirical correlation for narrow annuli at low mass velocity was then developed which has a good agreement with the experimental data.

Keywords: post-dryout; narrow annuli; low flow condition

1. Introduction

Post dryout heat transfer is of ever increasing importance particularly in the design of steam generators, nuclear reactor cooling systems, spray coolers, cryogenic equipment, quenching processes in metallurgy and other industrial applications. Various workers over the past decades attempted to explain post dryout heat transfer through identification of individual mechanism. Laverty and Rohsenow (1964) began with a two steps model that included vapor superheating at the wall and vapor cooling due to liquid evaporation in the free stream. The liquid phase was represented by a homogeneous mixture of spherical droplets. Forslund and Rohsenow (1968) extended this model by including the direct wall to droplet heat transfer, a droplet splitting mechanism and an improved drag coefficient[1].

Various parametric studies by Nijhawan et al .(1980), Nelson(1980), Yarkho et al.(1980), Yao & Rane (1980), and Michiyoshi & Makino(1979) have indicated that the degree of non- equilibrium and heat transfer characteristics of the liquid droplets play major roles in determining overall heat transfer rates and subsequent wall temperatures[1].In the post dryout region, after the film has dried out, Bennett et al.(1967)[2] identified heat transfer from the wall to the vapor and evaporation of droplets in the superheated vapor as the important mechanism determining wall temperature. Liquid droplets enhance the heat transfer after dryout or quench front by the absorption of heat from wall and vapor[3].

The research on these objectives is currently a new active

area. Osamusali and Chang(1988)[4] performed air-water two phase flow experiments using horizontal annuli produced by placing rods of various diameters along the central axis of an acrylic tube 5.08 cm inner diameter, and can therefore be considered as large channels. The present work was undertaken to investigate forced convective heat transfer characteristics in narrow annular gap in an attempt to compare with Groeneveld[5], Polimik[5], Miropolskiy[5], and Slaughterbeck[5] correlations and to determine experimentally how the heat flux, mass flux and pressure influences on the wall temperature and heat transfer.

Nomenclature

A	flow area (m^2)
De	hydraulic diameter (m)
F	heat transfer area (m^2)
h	heat transfer coefficient ($W / m^2 {}^oC$)
k	thermal conductivity ($W / m {}^oC$)
Nu	Nusselt number
Pr	Prandtl number
Re	Reynolds number
Q	rate of fluid heat transfer (W)
q	heat flux to fluid (kW / m^2)
T	temperature (^oC)
u	velocity (m / s)
x	vapor quality
ρ	density (kg/m^3)
μ	dynamic viscosity ($N s / m^2$)

Subscripts

f	liquid
g	vapor
h	homogeneous
i	inner tube
m	mean
o	outer tube
w	wall
cr	critical

2. Experimental Facility and Data Analysis

2.1 Experimental Facility

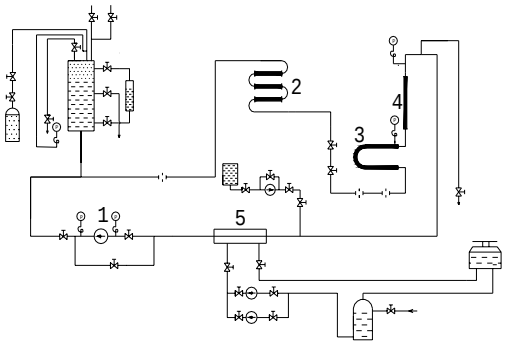

Fig.1. Experimental Test Loop

The experimental test loop is shown in Fig.1. The distilled water as working fluid entered water reservoir by passing negative ion exchanger resin, positive ion exchanger resin and mixture ion exchanger resin. It is drived by shield pump(1) and pass through S shape preheater(2), U tube shape preheater(3) and the vertical test section(4), then entered the condenser(5), finally returned to the shield pump.

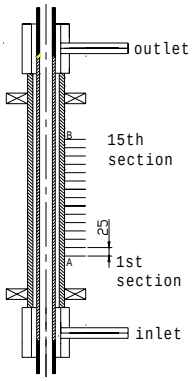

Fig.2 1.2 mm gap test section

The experimental test section is shown in Fig.2. The test section consists of outside tube and inside tube, which were made of specially processed straight stainless steel. The heated length of test section is 700 mm in length, the inner diameter of outside tube is 10.4 mm and thickness in 2.0 mm. The outer diameter of inside tube is 8.0 mm and thickness in 1.5 mm. Furthermore, in order to easily replace the test section a 'Swagelok' design in conjunction with standard stainless steel tee joint has been used to connect the rest of the test loop.

To keep concentricity in this narrow annulus and keep the outside and inside tube not contact each other, very small 3 ceramic rods (2.0 mm in diameter and about 1.1~1.2 mm in length) were arranged at the same cross section with equal angular interval at the upper and lower part of test section near the outlet and inlet. High temperature fluid flowed through annular channel, which was heated by direct two 100 kW power supplies to the outside and inside tube separately. In order to measure mass flux, pressure, temperature and the heat power, some measuring equipment and instruments were set up via IMP 35951 C data acquisition system, which sent into computer to display and record. There are 45 test points in the test section. Thirty thermocouples (0.5 mm in diameter) were welded on the outer surface of the outside tube to measure the outer wall temperature of outside tube. There are 15 cross sections measured along outside tube length direction, and the interval between two measuring adjacent cross section is 25 mm. In every cross section measured around the outside tube,

each 2 thermocouples were welded on the opposite side of the outside tube. In order to determine the inner wall surface temperature of the inside tube, sheathed thermocouple assembly that is composed of 15 thermocouples (0.5mm in diameter) were inserted in the inside tube at the same vertical level of the thermocouples on the outer surface of the outside tube. The thermocouples were wrapped by thin flexible mica for insulation with the inside tube that was filled with BN powder. The inlet and outlet fluid temperature of test section were measured by each thermocouple. The pressure was measured by using piezo capacitive type transducer. The flow rate of working fluid was measured by using a specialized orifice or venturi meter for low flow rate. All experimental data were installed to the data acquisition system. The steady state condition was reached when all the parameters reading by data logger remained a quantitative indication by using for instance the standard deviation value for a period of at least 30 minutes.

2.2 Experimental Data

The parametric range of experiment was as follow;

Pressure	1.39~5.90 (MPa)
Mass velocity	52.90~84.20 (kg / m^2 s)
Reynolds number	4415.20~7339.06
Heat flux (outside tube)	4.07~21.31 (kW / m^2)
Heat flux (inside tube)	3.90~25.20 (kW / m^2)
Mass quality	0.60~0.95

The parameters used in the data reduction and analysis were summarized below;

The heat transfer coefficient, $\mathbf{h = q / (T_w - T_s)}$

The heat power density of fluid was calculated as;

$\mathbf{q_i = Q_i / F_i}$ and $\mathbf{q_o = Q_O / F_O}$

Mean heat power density is-

$\mathbf{q_m = (Q_o + Q_i) / (F_o + F_i) = (q_o F_o + q_i F_i) / (F_o + F_i)}$

where Q_O, Q_i:heat power of outside and inside tube and

$F = \pi . d. L$

The inner surface temperature of the outside tube, T_{woi}, and the outer surface temperature of the inside tube, T_{wio}, are calculated from the measured outer surface temperature of the outside tube, T_{woo}, and the measured inner surface temperature of the inside tube, T_{wii}.

To get the inner surface temperature of outside tube T_{woi} from the measured outer surface temperature of outside tube T_{woo}, conduction in a column with average heat sources is evaluated and the final result is written as follows:

$$T_{woi} = T_{woo} - \left(\frac{q_o}{k_w}\right)\left(\frac{d_{oi}}{\left(d_{oo}^2 - d_{oi}^2\right)}\right)\left(\frac{d_{oo}}{2}\right)^2 \times \left[2\ln\left(\frac{d_{oo}}{d_{oi}}\right) + \left(\frac{d_{oi}}{d_{oo}}\right)^2 - 1\right]$$

Similarly, the outer surface temperature of inside tube T_{wio} can calculate from measured T_{wii}.

In the investigation of experiments, the fluid was at the thermodynamic non-equilibrium state, the steam was superheated and its temperature would not be measured in our study. Therefore, as some model exposed, the steam temperature was referred to as saturation temperature. For given mass flow, pressure and inlet quality, the heat flux are increased both on inside and outside tube until the desired value in bilaterally heating. On the other hand, the heat flux also can be increased only on the inside or outside tube in unilaterally heating. Usually, dryout did not occur at the same position along the inside and outside tube, it is depend on the condition of dryout appearance. The different temperature values of inside and outside tubes are due to the different post dryout status.

2.3 Experimental uncertainties

The uncertainties of the current is ±0.6% and voltage measurement is ±1.5%. The error in the dimension measurements is less than 1.0%. The thermocouples with an accuracy of ± 0.75% is utilized to measure both fluid and wall temperature. Other uncertainties are estimated as follow; ±0.25% for mass flow rate, ±0.25% for the pressure, 1.62% for the heat flux, and ±2.54% for the experimental efficiency. The maximum uncertainty for the heat transfer coefficient is ±1.528% and the random uncertainty of Nusselt is expected to be less than ±1.529%.

2.4 Post dryout heat transfer analysis

In the aspect of forced convective post dryout heat transfer, there were many kinds of empirical correlations. They generally predict a heat transfer coefficient based on the temperature difference between wall and saturation. These are simple to use but have a limited range of validity. The following Groeneveld, Miropolskiy, Polomik and Slaughterbeck correlations were used in the experimental analysis.

(1) Groeneveld correlation[5] fitted pressure 3.4~10.0 MPa, and mass flux 800~4100 kg /m^2 s for annuli.

$Nu_g = 0.052\{ Re_g [x + \rho_g/\rho_f (1 - x)] \}^{0.688} Pr_w^{1.26} \; Y^{-1.06}$

where $Y = 1- 0.1 (\rho_f/\rho_g -1)^{0.4} (1- x)^{0.4}$

(2) Miropolskiy correlation[5] fitted pressure 4.0~22.0 MPa and mass flux 700~2000 kg /m^2 s for tubes.

$Nu_g = 0.023\{ Re_g [x + \rho_g/\rho_f (1 - x)] \}^{0.8} Pr_w^{0.8}$ Y

where , Y is the same as (1).

(3) Polomik correlation[5] fitted pressure 4.0~10.0 MPa and mass flux 700~2700 kg /m^2 s for 2 rods geometry.

$Nu_g = 0.00115\ Re_g^{0.9} Pr_g^{0.3} [(1.8T_w+32) / (1.8T_s+ 32) - 1]$

(4) Slaughterbeck correlation[5] fitted 6.8~20.0 MPa and mass flux 1050~5300 kg /m^2 s for tubes.

$Nu_g = 1.16 \times 10^{-4} \{ Re_g [x + \rho_g/\rho_f (1 - x)] \}^{0.838} Pr_w^{1.81} q^{0.278} (k_g / k_{cr})^{-0.508}$

where , k_{cr} = 0.914 W /m ℃ (critical thermal conductivity)

According to above mentioned four correlations, we got four calculated correlations on the experimental data from relevant original correlations in low mass flux. The comparison between original and obtained coefficients were as below-

Fig. No	Correlation	original coeff:	Obtained coeff:
3	Groeneveld	0.052	0.028
4	Miropolskiy	0.023	0.021
5	Polomik	0.00115	0.0052
6	Slaughterbeck	1.16x 10^{-4}	1.882x 10^{-4}

From Figures 3 to 6, we can see that original coefficients of Groeneveld (Fig.3) and Miropolskiy (Fig.4) correlations were bigger than obtained coefficients on the experimental data. On the other hand, the original coefficients of Polomik (Fig.5) and Slaughterbeck (Fig.6) correlations were smaller than obtained coefficients on the experimental data. Apparently, it was different from the result of original empirical correlations. That was very complicated for post dryout forced convective heat transfer in narrow annular channel. It was well known that, in general, the assumption of thermal equilibrium in the post dryout forced convective heat transfer is not appropriate.

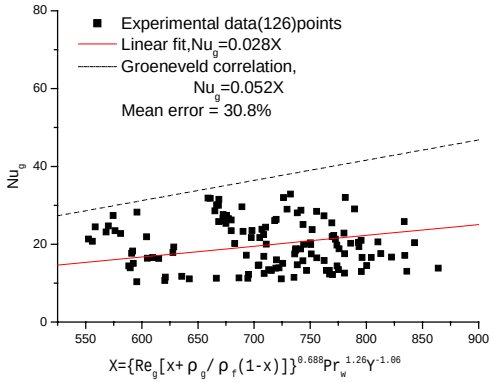

Fig.3 Groeneveld correlation linear fit

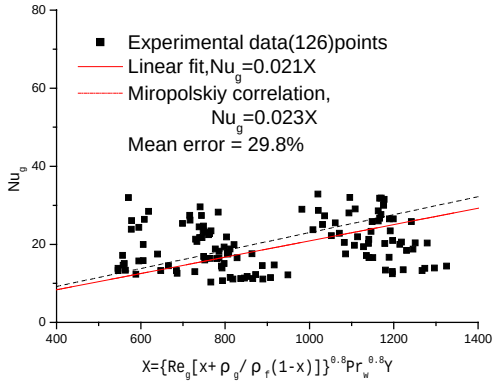

Fig.4 Miropolskiy correlation linear fit

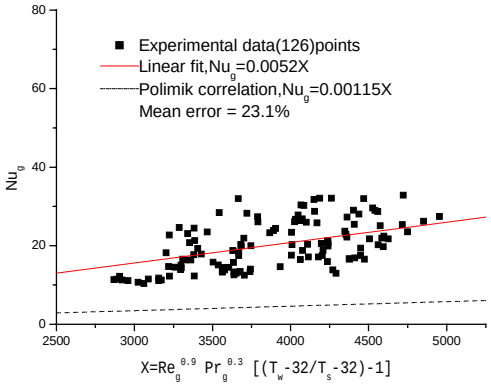

Fig.5 Polimik correlation linear fit

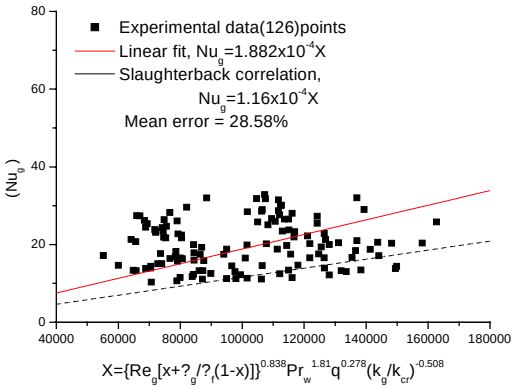

Fig.6 Slaughterbeck correlation linear fit

3.0 The factor analysis on the wall temperature

3.1 Effect of heat flux

The wall temperature of inside and outside as a function of the two different heat flux are shown in Fig.7. For a given heated length, the wall temperature increases with increasing heat flux. Heat transfer in a post dryout flow regime involves various heat exchange path among the vapor phase, droplets and the heated wall. The liquid is assumed in thermal equilibrium with the vapor, and the heated surface is cooled by forced convection of the vapor only. However, at

low–medium pressure and low mass flux, thermal non-equilibrium is more obvious. The higher wall temperature, due to the higher heat flux, results in a higher convective heat transfer coefficient.

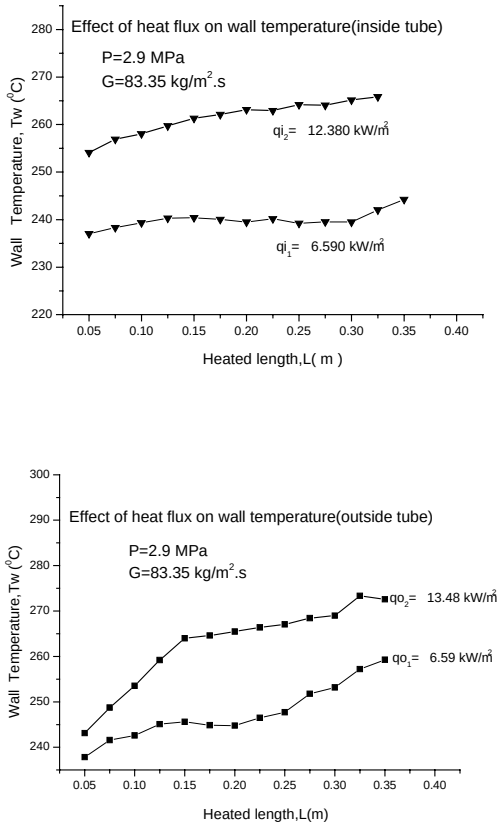

Fig.7 Effect of heat flux on wall temperature

3.2 Effect of pressure

Figure.8 presents the wall temperature results as a function of the heated length for two different pressures. Examining this figure, it can be seen that the wall temperature decreases with the increase of the pressure. As the pressure increases, the wall temperature decreases and the vapor convective heat transfer becomes big since this quantity is calculated based on the heat flux and the temperature difference between saturated and heated wall. As a consequence, the heat transfer coefficient increased.

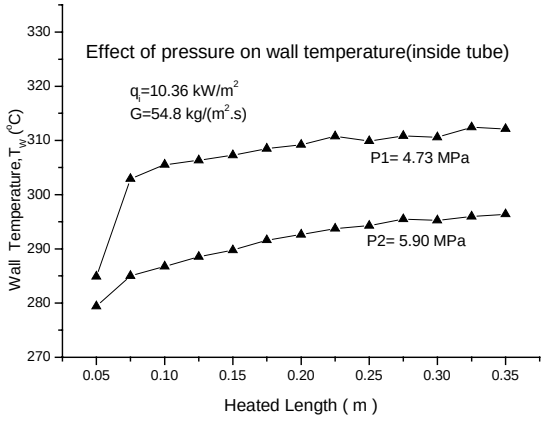

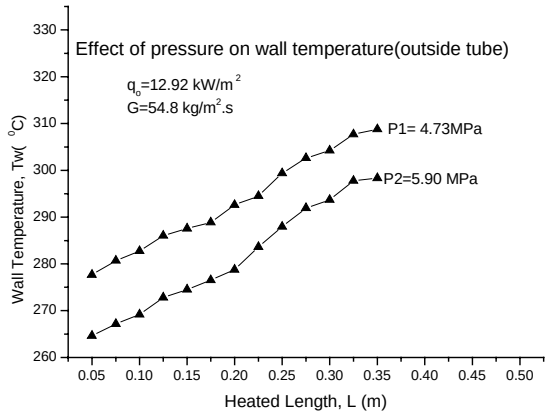

Fig.8 Effect of pressure on wall temperature

3.3 Effect of mass velocity

As shown in Fig.9, the wall temperature decreases with increasing the mass velocity. At fixed heat flux and inlet temperature of working fluid, the increase of mass velocity causes the decrease of outlet temperature of fluid and then wall temperature decreased. In short, as the mass velocity increases, heat transfer process such as wall to vapor, wall to droplets and vapor to droplets improved. Thus, the heat transfer coefficient increased.

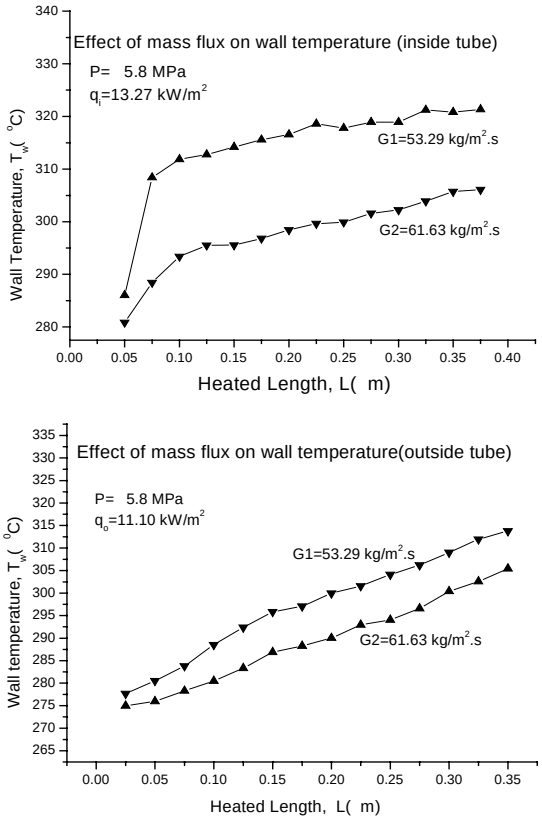

Fig.9 Effect of mass velocity on wall temperature

4. Development of the new correlation

Based on the heat transfer analysis and the effects of heat flux , mass flux and pressure on the wall temperature,

Groeneveld correlation form was modified in conjunction with temperature effect portion from Polomik correlation. In the post dryout region, the important mechanism of heat transfer from the wall to the vapor and evaporation of droplets in the superheated vapor determined the wall temperature. The liquid is assumed in the thermal equilibrium with the vapor, and the heated surface is cooled by forced convection of the vapor only. At the same time, as vapor's radial velocity was not uniformity, there were random colliding between liquid droplets which made the movement of liquid droplets at random and collide to the wall. Because such collision made droplets break seriously, the temperature of outside and inside wall had a significant influence on the heat transfer of the annular channel. For this reason, temperature effect portion was used in the new correlation. After considering the influence of wall temperature on the annular gap, a polynomial fitting was processed, as shown in Fig.10. The equation of polynomial fitting was below:

$$Nu_g = 1.4x\,10^{-4}\{ Re_g [x + \rho_g/\rho_f (1 - x)] \}^{1.243} \; Pr_w^{0.766} \; Y^{0.916} (T_w / T_s - 1)^{-0.659}$$

where, $Y = 1 - 0.1 (\rho_f/\rho_g - 1)^{0.4} (1 - x)^{0.4}$

The experimental data used in the comparison total cover a parametric range of P =1.39~5.9 MPa, G =52.90~84.20 kg /m^2 s and x = 0.6~0.95. Within this range, the predicted data shows good agreement with the experimental data on the Nusselt number of vapor. The mean error for the experimental data compared is 12.31 % (see Fig.10).

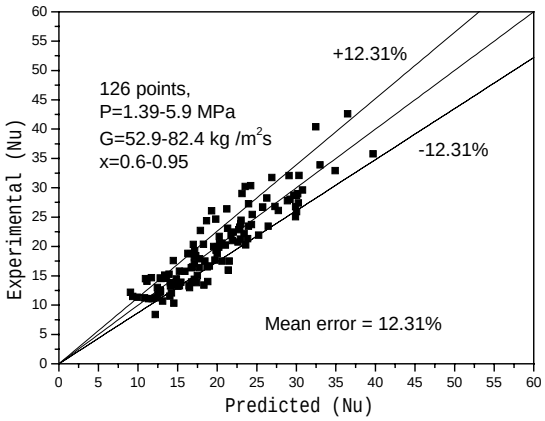

Fig.10 Comparison of Nu number

4. Conclusion

In this paper the forced convective post dryout heat transfer in annular channel with 1.2 mm gap was experimentally investigated. On the base of the comparison and analysis of the four empirical correlations such as Groeneveld, Miropolskiy, Polomik and Slaughterbeck, the results show that the prediction of post dryout heat transfer was uncertain for low mass velocity. At condition of lower mass velocity, the droplets are larger in diameter; the interfacial heat transfer is inefficient and the vapor is thus highly superheated. The vapor phase superheat, which is determined by a competition of various components of heat transfer taking place among the droplets, the vapor phase and the heated wall, may reach high temperature degrees. This phenomenon has made the prediction of post dryout heat transfer flow regime more complicated and more difficult. Because of this reason, exact mechanism for the heat transfer processes are still poorly understood and reliable prediction methods are still being need to be carried out. This paper suggested a new empirical correlation in the parametric range of P= 1.39~5.9 MPa, G= 52.9~84.2 kg /m^2 s and x= 0.6~0.95. It was good agreement with the experimental data and heat transfer coefficient increases with increasing of heat flux, mass flux and pressure.

References

1. Moose, R.. A. & Ganic', E. N. On the calculation of wall temperatures in the post dryout heat transfer region, Int. J. Multiphase Flow Vol.8, No.5 (1982) 525-542
2. A.W.Bennett.G.F.Hewitt.H.A.Kearsey and R.K.F.Keeys. Heat transfer to steam water flowing in uniformly heated tubes in which the critical heat flux has been exceed. UKAEA Report AERE R5373(1967)
3. H.Y. Jeong and H.C. No, Modelling for post dryout heat transfer and droplets sizes at low pressure and low flow conditions, Int.Comm.Heat Mass Transfer, Vol.23, No.6 (1996)767-778
4. Osamusali S.I and Chang J.S, Two phase flow regime transition in a horizontal pipe and annulus flow under gas-liquid two-phase flow, ASME FED, Vol. 72 (1988) 63-69.
5. D.C, Groeneveld, Post dryout heat transfer; physical mechanism and a survey of prediction methods, Nuclear Engineering and Design 32(1975)283-294.
6. B.J.Azzopardi, Prediction of dryout and burnout heat transfer with axially non-uniform heat input by means of an annular flow model, Nuclear Engineering and Design 163(1996)51-57.
7. R.L.Liu and D.N.Jia, Experimental Investigation on Post Dryout Dispered Flow Heat Transfer in an Annular Gap, Proc. of International Conference on Power Engineering, Xi'an,2001.